Korea-Australia Rheology Journal
Vol. 23, No. 2, June 2011 pp. 81-87
DOI: 10.1007/s13367-011-0011-9

Application of geometric algorithm of time-temperature superposition to linear viscoelasticity of rubber compounds

Jung-Eun Bae[1], Kwang Soo Cho[1,*], Kwan Ho Seo[1] and Dong-Gug Kang[2]
[1]*Department of Polymer Science and Engineering, Kyungpook National University, Daegu, Korea*
[2]*Research and Development Institute, Pyung-hwa Oil Seal Industry Co. LTD., Daegu, Korea*
(Received January 31, 2011; accepted March 13, 2011)

Abstract

We tested usefulness of a new algorithm of time-temperature superposition to linear viscoelasticity of three kinds of rubber compounds which are conventional in rubber industries. Different from viscoelastic fluids, linear viscoelasticity of rubber compounds are usually measured by temperature-sweep test at fixed frequencies. We converted the viscoelastic data as functions of temperature to those as functions of frequency. We also investigated effect of rubber structures on their linear viscoelasticity.

Keywords **:** time-temperature superposition, rubber compounds, linear viscoelasticity

1. Introduction

Time-temperature superposition (TTS) is a useful tool to remove the limitation of measurement range of linear viscoelasticity (Ferry 1980). TTS allows the collection of data measured at various temperatures but limited frequency range to be transformed to the ones over a wide range of frequency at an arbitrary temperature. As for conventional viscoelastic fluids such as polymer melts, linear viscoelasticity can be measured as a function of frequency (or time) at a given temperature, while it is nearly hard in the case of viscoelastic solids such as plastics and rubbers to measure their viscoelasticity as a function of frequency because most available instruments for viscoelastic solids have the limitation to control frequency to be wanted.

Most popular instruments for linear viscoelasticity of solids control temperature instead of frequency at a few frequencies. However, in design of mechanical units made of viscoelastic solids, relaxation modulus is preferred to dynamic modulus as a function of temperature. Hence, it is important to convert dynamic modulus as a function of temperature to relaxation modulus as a function of time at a temperature under consideration, in industries. For this conversion, two steps of data processing are required. The first step is to convert dynamic modulus as a function of temperature to the one as a function of frequency. The next step is to convert the dynamic modulus as a function of frequency to relaxation modulus. In the first step, TTS is used while calculation of relaxation spectrum is required in the second step.

Recently, Cho (2009) developed a new algorithm for time-temperature superposition (TTS) which is based on the minimization of arc length of data. Only concept and an example of the algorithm are described in the paper of Cho (2009). The example used in the paper is the data of polymer melt. In this paper, we describe and test the algorithm in detail for simulated data and experimental data of rubber compounds. We also investigated the effects of structures of rubber compounds on their linear viscoelasticity.

2. Algorithm of TTS

Consider the time-temperature superposition of linear viscoelastic data such as dynamic moduli as functions of frequency measured at various temperatures:

$$G'(\omega, T) = b_T G'(a_T\omega), \quad G''(\omega, T) = b_T G''(a_T\omega) \tag{1}$$

We can determine the horizontal shift factor, a_T first and then the vertical shift factor, b_T. When we consider the plot of loss tangent as a function of frequency, the plot is independent of the vertical shift factor because of the definition of the loss tangent:

$$\tan\delta(\omega, T) = \frac{G''(\omega, T)}{G'(\omega, T)} = \frac{G''(a_T\omega)}{G'(a_T\omega)} \tag{2}$$

Cancelation of the vertical factor can be achieved equivalently for cosδ, sinδ, cotδ too. After the determination of the horizontal shift factor from the plot of loss tangent, we can determine the vertical shift factor from the plot of one of the dynamic moduli as a function of frequency. Hence, we explain the algorithm of the minimum arc length by only consider the case of horizontal shift factor.

Assume that the moduli are measured at n+1 temper-

*Corresponding author: polphy@knu.ac.kr
© 2011 The Korean Society of Rheology and Springer

atures, say $T_0 < T_1 < \cdots < T_n$, and the number of frequency, m is the same for all temperatures. Without loss of generality, we set the reference temperature the lowest temperature, T_0. From the experiment, we have n sets of data $((\omega, \tan\delta))$. For convenience, we use the notation ω_i^k and $\tan\delta_i^k$ where the subscript i stands for the index of frequency and the superscript k for that of temperature, respectively. As the first step, we consider two sets of data obtained from the first two temperatures, T_0 and T_1. Multiply an assumed shift factor A_1 by m frequencies ω_i^1 and arrange the two data sets, $(\omega_i^0, \tan\delta_i^0)$ and $(A_1\omega_i^1, \tan\delta_i^1)$ in the ascending order of ω_i^0 and $A_1\omega_i^1$. In other words, we denote W_1 as the lowest frequency among the $2m$ frequencies such as ω_i^0 and $A_1\omega_i^1$ and W_{2m} as the highest frequency. Of course $\tan\Delta_p$ is the loss tangent for W_p. Thus we need a sorting process for rearrange the two sets of data from temperature T_0 and T_1. Then we can calculate the arc length such that

$$S_1(A_1) = \sum_{p=2}^{2m} \sqrt{(\log W_p - \log W_{p-1})^2 + (\log\tan\Delta_p - \log\tan\Delta_{p-1})^2} \quad (3)$$

It is straightforward that the arc length has the global minimum at a certain value of A_1. Since there are several numerical methods have been developed for the minimization of a function of single variable, it seems to be easy to determine the optimum shift factor. However, most conventional algorithms fail to find the optimum shift factor because the arc length as a function of A_1 usually has so many local minima. It will be shown later. At any rate, it is not difficult to find a numerical method suitable for this problem. We refer the optimum shift factor to A_1^*.

Next step consists of [1] the multiplication of a test shift factor A_2 to ω_i^2, [2] combining the data of temperature T_2 with previously obtained data set $(W_k, \tan\Delta_k)$ with k running from 1 to $2m$, [3] sorting the combined $3m$ data points in the order of the rescaled frequency, and [4] determination of the minimum arc length of the $3m$ data points. In this case, the arc length is given by

$$S_2(A_2) = \sum_{p=2}^{3m} \sqrt{(\log W_p - \log W_{p-1})^2 + (\log\tan\Delta_p - \log\tan\Delta_{p-1})^2} \quad (4)$$

It is noteworthy that we assign W_p to the pth lowest frequency among ω_i, $A_1^*\omega_i^1$ and $A_2^*\omega_i^2$ and $tan\Delta_p$ to the corresponding loss tangent. We denote the shift factor A_2^* as the one that makes the arc length of Eq. (4) minimum. Repeating this procedures for the rest temperatures gives the set of shift factors $A_0^* = 1, A_1^*, A_2^*, \ldots, A_n^*$. If we consider the reference temperature $T_R = T_q$, then it is easily understood that

$$a_{T_k} = \frac{A_k^*}{A_q^*} \quad (5)$$

Vertical shift factor can be determined in a similar manner. In this case, we use the plot of $a_T\omega$ as a function of G'.

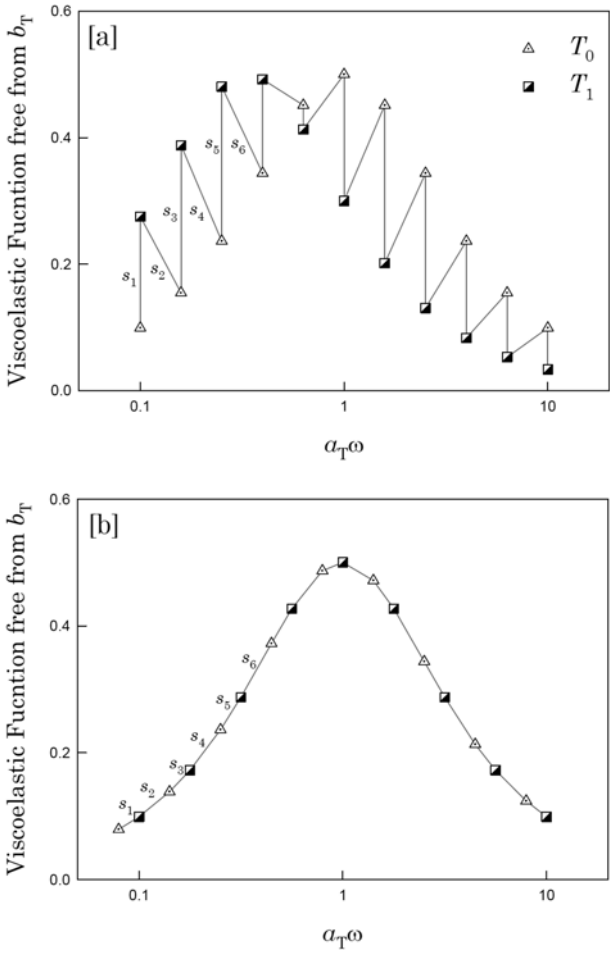

Fig. 1. The concept of minimization of arc length.

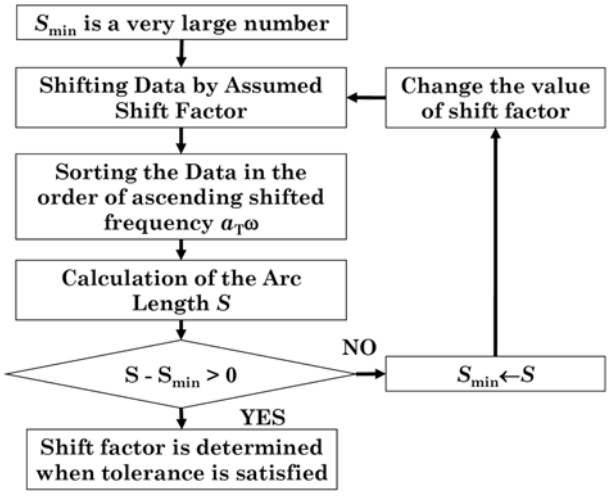

Fig. 2. Flow chart of the algorithm.

It is better to use storage modulus instead of loss modulus, because storage modulus is an increasing function of frequency while loss modulus is not. Thus we do not have to describe the procedure for vertical shift factor in detail.

Fig. 1 shows how the arc-length minimization can determine shift factor in a schematic manner. Fig. 1[a] stands for incomplete superposition whose arc length is larger than that of complete superposition shown in Fig. 1[b]. Fig. 2 shows the algorithm in terms of flow chart.

Another version of the algorithm is to use WLF equation such that

$$a_T = \exp\left[\frac{-c_1(T-T_r)}{c_2+T-T_r}\right] \tag{6}$$

where c_1 and c_2 are constants of WLF equation and T_r is the reference temperature. We multiply a_T of Eq. (6) to frequencies of corresponding temperature and minimize the arc length of loss tangent or its alternatives with varying the values of c_1 and c_2.

3. Test of the Algorithm by Simulated Data

We generated a set of linear viscoelastic data from the following equations:

$$G^*(\omega)G_e\left(\frac{i\lambda_1\omega}{1+i\lambda_1\omega}+\rho\frac{i\lambda_2\omega}{1+i\lambda_2\omega}\right) \tag{7}$$

$$\lambda_1 = \lambda_1^{(0)}\Lambda(T),\ \lambda_2 = \lambda_2^{(0)}\Lambda(T) \tag{8}$$

$$\Lambda(T) = \exp\left(-\frac{c_1(T-T_0)}{c_2+T-T_0}\right) \tag{9}$$

where $G_e = 1$, $\rho = 100$, $\lambda_1^{(0)} = 1$, $\lambda_2^{(0)} = 0.001$, $c_1 = 10$ and $c_2 = 50$ were used. We generated five data sets for temperatures of T = 100, 120, 140, 160, and 180°C in the frequency range such that $\log_{10}\omega_n = -1+0.2n, n = 0,1,\ldots,12$. Note that $T_0 = 100°C$ was used in Eq. (9). From Eqs. (7)~(9), it is clear that the plots of viscoelastic functions such as storage and loss moduli as functions of frequency can be superposed on a single curve when frequency w is replaced by $\Lambda(T)\omega$. It is remarkable that we did not contain any vertical shift in the simulated data.

Since the simulated data have no experimental error, it is easy to check how the algorithm of minimum arc length is efficient. Fig. 3 (a) is the plot of cotδ as a function of ω and Fig. 3(b) is the corresponding master curve which is obtained by the optimum shift factor. Fig. 4 shows the results that are obtained when full-search algorithm for minimum arc length is used. The arc length as a function of horizontal shift factor shows several local minima although it also shows the global minimum. Hence, gradient type minimization may be trapped in a local minimum which must not be the global minimum. A minimization algorithm may suffer from severe initial-value dependence. However, suitable initial condition can be easily estimated because it can be considered as the average distance between the data points of two temperatures which have the same height. The estimated shift factor is usually located near the global minimum.

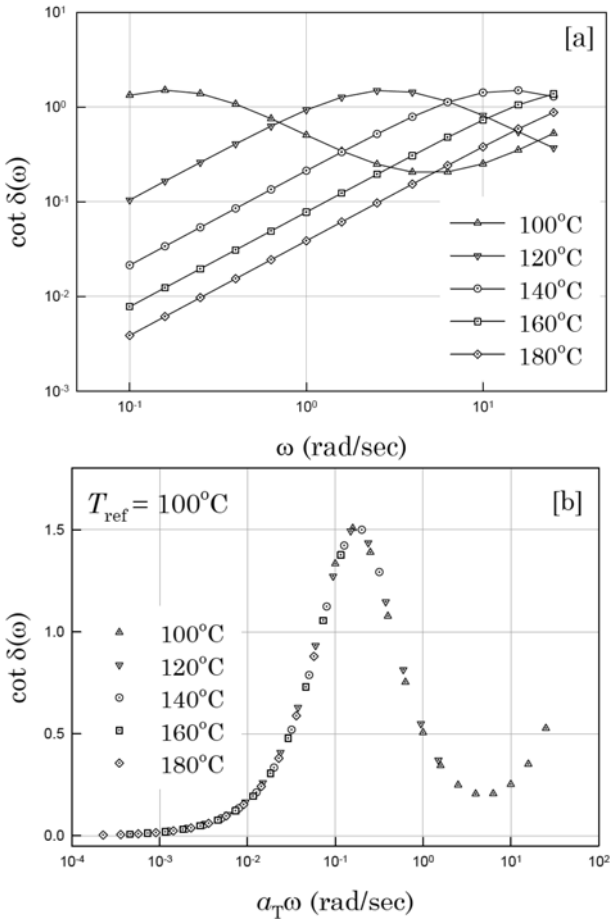

Fig. 3. Simulated data and their superposition.

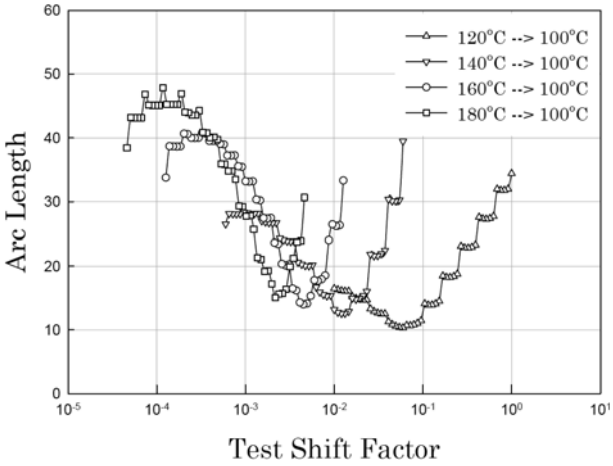

Fig. 4. Map of arc length as a function of test shift factor.

Consider two sets of data measured at two different temperatures, T_0 and T_1. If the data sets for a viscoelastic function f, satisfy time-temperature superposition, there exists overlap region where some of (ω_i^0, f_i^0) and some of

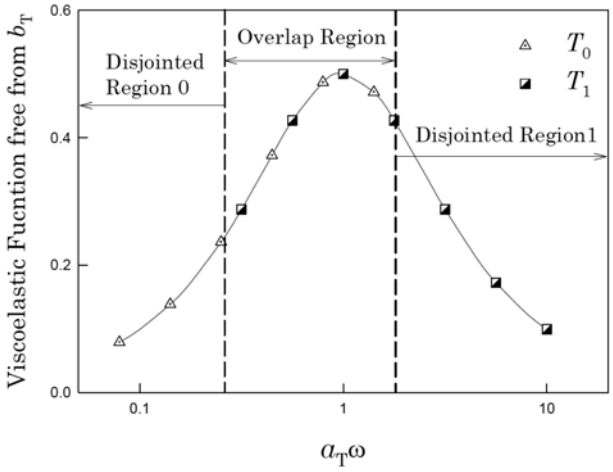

Fig. 5. A schematic diagram for explanation of several local minima in Fig. 4.

$(a_{T_1}\omega_k^1 f_k^1)$ overlap as shown in Fig. 5. Outside of the overlap region there are two disjoint regions: one for T_0 and the other for T_1. The total arc length is the sum of the partial arc lengths of the three regions. We call L_0 and L_1, respectively, the partial arc lengths of the two disjoint regions and call L_{overlap} the partial arc length of the overlap region. As the test shift factor changes, the frequency range of the three regions increases or decreases. Assume that the number of frequencies of the two data sets are equal and for all $i = 1, 2, \ldots, m, \omega_i^0 = \omega_i^1$. Because of $T_1 > T_0$, we changes the test shift factor from unity to smaller number. When the test shift factor is unity, there is no disjoint region and the total arc length S is given by $S = L_{\text{overlap}}$. As the test shift factor decreases from unity, L_{overlap} decreases and both L_0 and L_1 increase from zero, while the total arc length decreases. When increase in the sum of the arc lengths of the disjoint regions overcomes decrease in L_{overlap}, the total arc length becomes increasing. Then we have local minimum in the total arc length. After passing the local minimum, the decrease in L_{overlap} overwhelms the increases in $L_0 + L_1$, which makes S decrease again. Repetition of this competition between the partial arc lengths continues until the test shift factor arrives at the optimum. After passing the optimum, the length of frequency range of overlap continuously decreases while L_{overlap} increases because of the increases in incompleteness of superposition. Hence the total arc length increases again. This reasoning explains the several local minima in Fig. 4.

Fig. 6 shows the optimum shift factors obtained by the algorithm shown in Fig. 2. The continuous line in Fig. 6 is $\Lambda(T)/\Lambda(T_0)$ which is the exact shift factor. In the algorithm, we moved the test shift factor in logarithmic scale with a suitable step size. After obtaining pseudo minimum by the logarithmic move of the test shift factor, we searched the optimum shift factor in linear scale around the pseudo minimum. After finding the optimum shift factor for T_1, the procedure for the optimum shift factor of T_2 starts. In this case, the reference curve is the superposed curve obtained from the data of T_0 and T_1. Since the optimum shift factor of T_2 should be less than that of T_2, we decreased the test shift factor of T_2 from the value of the optimum shift factor of T_1.

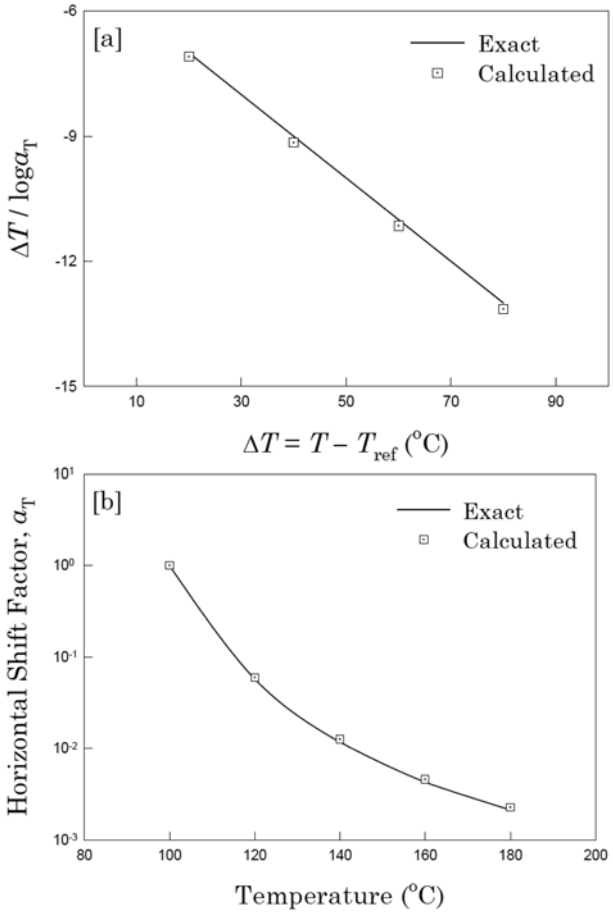

Fig. 6. Comparison of calculated and exact shift factors.

Since the speed of modern personal computer is high enough to give expected results in a few second even though the algorithm consists of several sorting and summing, full searching used in this algorithm cannot be said inefficient from the viewpoint of numerical analysis. Other minimizing algorithm such as gradient method is not available because the total arc length shows several local minima as the test shift factor changes. Local minima play the role of trap in gradient method which cannot give correct optimum shift factor.

Compared with the method of Honerkamp and Weese(1993), our algorithm may be less efficient from the view point of numerical analysis. However, our algorithm does not have to assume the functional form of viscoelastic functions as Honerkamp and Weese(1993) used polynomial

Table 1. Composition and physical properties of rubber compounds

Rubber	EPDM			NBR			FKM		
Code	E1	E3	E5	N1	N3	N5	F1	F3	F5
C/B	0	30 phr	0	0	30 phr	0	0	30 phr	0
Si	0	0	30 phr	0	0	30 phr	0	0	30 phr
$T_a(K)$[1]	35960	29021	35676	33513	34122	39848	32360	29021	33448
$T_a(K)$[2]	22950	22300	25950	22350	25800	25750	25100	23800	22550

C/B: carbon black;Si: silica
[1]Activation temperature calculated from Eq. (12) and (13)
[2]Activation temperature determined by the minimization of arc length

in logarithmic scale. When the functional form of the master curve varies fast, the algorithm of Honerkamp and Weese(1993) should suffer from high order of the polynomial, which must result in low efficiency of the algorithm.

4. Experiment

4.1. Materials

We tested three kinds of rubbers that are produced commercially in Pyung-hwa oil seal: EPDM(ethylene propylene diene monomer copolymer), NBR(acrylonitrile butadiene rubber) and FKM(flouronated hydrocarbon rubber). We added two kinds of fillers such as silica and carbon black with identical curing conditions suitable for each rubber sort. Table 1 shows specification of the materials used.

4.2. Measurement

We used DMA Q800 (TA instruments) for measurement of linear viscoelasticity of the rubber compounds. We choose three frequencies: 0.1, 1, 10 Hz. The deformation mode was single cantilever. Heating speed was 2°C/min. We used liquid nitrogen to obtain temperature range from −100°C to 100°C.

5. TTS of Rubber Compounds

The temperature at which loss tangent becomes the maximum is considered as the glass transition temperature measured at a given frequency. EPDM samples have T_g around −33°C, NBR around −16°C, and FKM around +2°C. The effect of filler on glass transition temperature was negligible.

Since loss tangent shows a peak near glass transition temperature and frequency is fixed in the measurements by DMA, we can have

$$\frac{\mathrm{d}\tan\delta}{\mathrm{d}(a_T\omega)} = \frac{1}{\omega}\frac{\mathrm{d}\tan\delta}{\mathrm{d}T}\frac{\mathrm{d}T}{\mathrm{d}a_T} \tag{10}$$

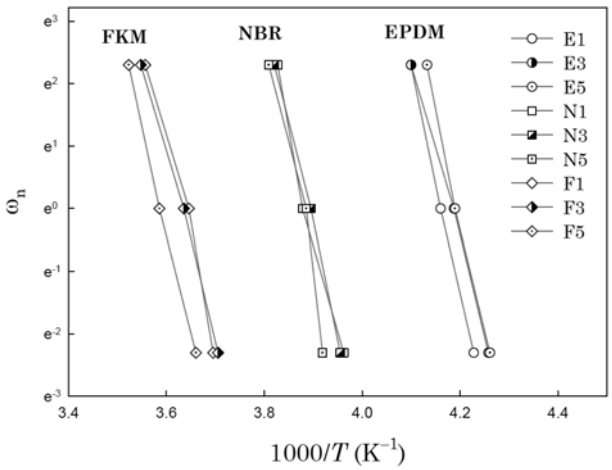

Fig. 7. The plot of measurement frequency and peak temperature.

It is easily understood that Eq. (10) becomes zero at glass transition temperature. If loss tangents are measured at several fixed frequencies, say $\omega_1,\ldots,\omega_n$, then it is clear that TTS implies

$$\omega_{\text{peak}} \equiv (a_T\omega)_{\text{peak}} = a_{T_1}\omega_1 = \ldots = a_{T_n}\omega_n \tag{11}$$

where ω_{peak} is the reduced frequency at the maximum loss tangent and T_n is the temperature at which loss tangent is the maximum when measurement is done at the fixed frequency ω_n. When reference temperature is fixed, it must be noted that ω_{peak} is fixed. Eq. (11) implies that

$$\log\omega_k = \log\omega_{\text{peak}} - \log a_{T_K} \quad \text{for } k = 1,2,\ldots,n \tag{12}$$

Hence Eq. (12) implies that when frequency is plotted against temperature, we can determine the temperature dependence of shift factor.

Glass transition temperature (T_g) of above rubbers are known to belong to the temperature range of measurements. Hence it is hard to use WLF equation for shift factor because WLF equation diverges around glass transition temperature. Instead of WLF equation, we may use Arrhe-

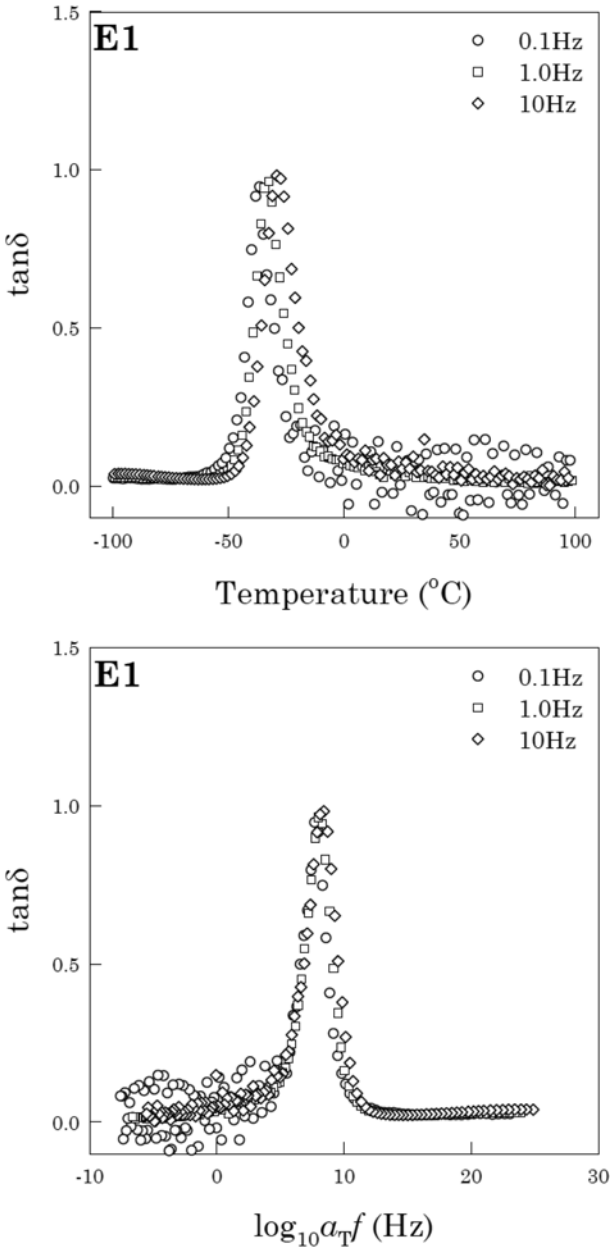

Fig. 8. Example of superposition by arc length minimization. The sample is E1 (EPDM) and the reference temperature is 25°C.

nious type equation as follows

$$a_T = \exp\left(\frac{E}{\mathrm{R}}\left(\frac{1}{T}-\frac{1}{T_r}\right)\right) \tag{13}$$

where R is the gas constant and E is the activation energy. Use of Eq. (13) seems valid from Fig. 7. The lines connecting symbols in Fig. 7 are eye-guides not regression results. From Fig. 7, we calculated activation temperature, $T_a \equiv E/R$ which are listed in Table 1. The activation temperatures are, of course, calculated by both regression with Eq. (12) and (13) and arc length minimization. Since filler is thought to be less effective on thermal relaxation process of rubber molecules, the variation of activation temperature according to addition of filler is expected to be small. Compared the two calculation of activation temperature, the arc length minimization seems to be better.

Fig. 8 shows an example of the superposition by arc length minimization. Since high temperature data has big noise, arc length minimization is applied to the data whose loss tangent is larger than 0.5. While use of Eqs. (12) and (13) consider only a single data point, the arc length minimization includes several data points. Hence, the arc length minimization can be thought as better one.

6. Effect of Rubber Structure on Linear Viscoelasticity

Fig. 9 is the collection of loss tangent data as functions of frequency. Since data measured at different frequencies overlap over wide range of reduced frequency and include the peak of glass transition, it is no loss of generality to use only 10 Hz data. Since 10 Hz data has, comparatively, less noise level, use of 10 Hz data is easier to investigate structure effect on linear viscoelasticity.

It is well known that EPDM has the lowest glass transition temperature, FKM has the highest glass transition temperature and NBR has intermediate, while cross linking density and other effect influence glass transition temperature. Fig. 9 shows that glass transition temperatures of the samples used here mainly depend on main chain properties irrespective of subtle difference in cross linking density. We did not measure cross linking density of the samples.

It is interesting that addition of fillers changes the maximum of loss tangent while shift of glass transition is comparatively small. In the case of EPDM, decrease of the height of loss tangent is larger when carbon black is added than when silica is added. However, in the case of FKM, addition of silica results in slight increase in the height of loss tangent while addition of carbon black causes much decrease of the height of loss tangent. In the case of NBR, difference between silica and carbon black does not appear while addition of filler reduces the height of loss tangent.

When connection between filler and polymer medium is strong, effect of filler on loss tangent is negligible. When the connection is so weak to induce slip in the interface, loss tangent of filled polymer may be higher than that of non-filled polymer. The connection of filler with rubber polymer depends on both interactions between filler particles and polymer chains and degree of wetting of polymer chains on filler surface. The wetting depends on viscosity and rate of curing during the mixing process in manufacture of final rubber compounds. While carbon black has a lot of active sites where rubber polymer chain can be captured, silica does not. Hence, silica has positive effect in the height of loss modulus compared with carbon black. Since FKM

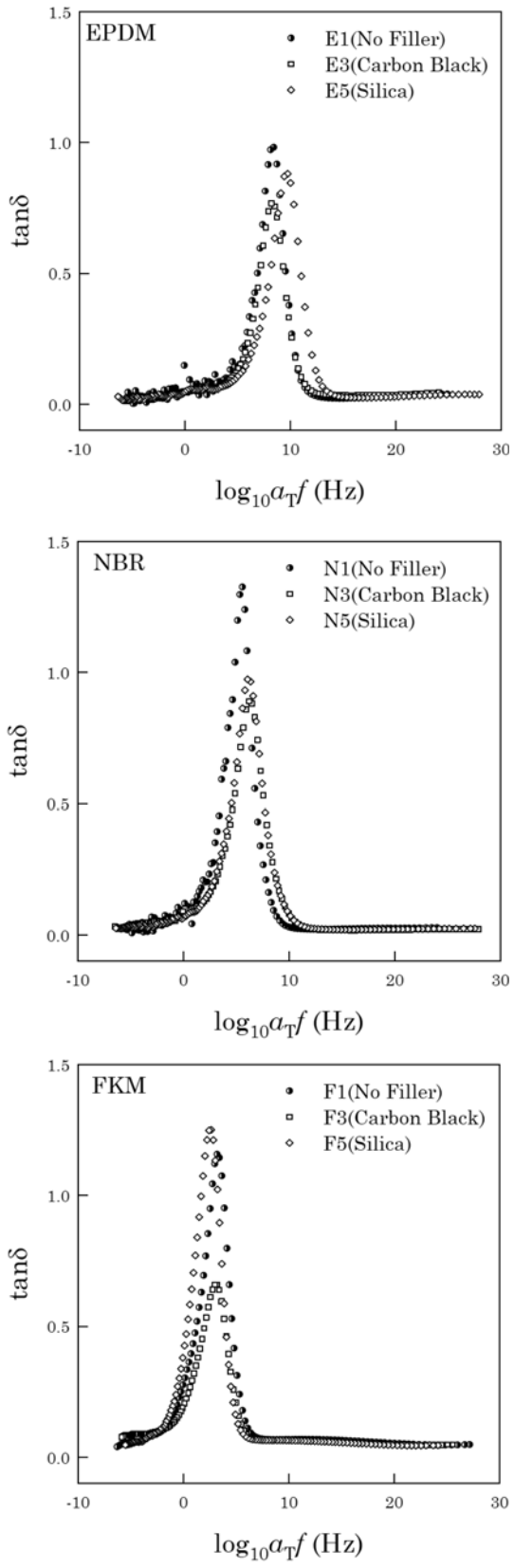

Fig. 9. Loss tangent of rubber compounds as a function of reduced frequency. Effect of filler is outstanding in the case of FKM compared with other rubbers.

has higher viscosity and higher glass transition temperature than other rubber polymers, wetting of FKM on silica particle is poorer than those of EPDM and NBR. These explain why loss tangent of F5 is higher than that of F1. Considering polarity of rubber molecules, EPDM can be classified as a non-polar molecule, FKM has highest polarity and NBR is between FKM and EPDM. The active site of carbon black consists of acid groups or others which may form hydrogen bonds or alike with FKM. This seems to explain why loss tangent of F3 has much lower than that of F1.

Carbon black particle is a cluster of nano particles while diameter of silica particle is order of micro meter. Loading content of 30 phr is enough to increase of modulus of rubber compounds. In this loading content, modulus increases significantly by addition of filler particle whose modulus is higher than the medium. Effect of carbon black on equilibrium modulus (modulus at infinitely high frequency, E'_∞) is equivalent to increase of cross linking density due to connection of chains via carbon black particles. On the other hand, addition of silica is hard to expect any increase of cross linking density. Silica has higher modulus than rubber medium. Hence, addition of silica increases E'_∞ much higher than that of carbon black as shown in Table 1.

7. Conclusions

We tested geometric algorithm of TTS with simulated data of conventional viscoelastic fluids and applied successfully it to real data of rubber compounds whose shift factor is different from WLF equation. The algorithm is based on the minimization of arc length of viscoelastic functions. The algorithm for rubber compounds is superior to conventional method based on Eqs. (12) and (13), because the activation temperatures calculated by arc length minimization are more realistic than its counterpart.

From the TTS by arc length minimization, we learned effect of structure on linear viscoelasticity of composite rubber compounds.

Acknowledgement

This research was financially supported by the Ministry of Education, Science Technology (MEST) and Korean Institute for Advancement of Technology (KIAT) through the Human Resource Training Project for Regional Innovation.

References

Cho, K. S., 2009, Geometric interpretation of time-temperature superposition, *Korea-Austalia Rheol. J.* **21**, 13-16.

Ferry, J. D., 1980, *Viscoelastic properties of polymers*, John Wiley & Sons, New York.

Honerkamp, J. and J. Weese, 1993, A note on estimating mastercurves, *Rheol. Acta* **32**, 57-64.